



Published in final edited form as:

Immunohorizons. ; 3(12): 593–605. doi:10.4049/immunohorizons.1900045.

Development of Type 2 Innate Lymphoid Cells Is Selectively Inhibited by Sustained E Protein Activity

Hannah Berrett^{*,†}, Liangyue Qian^{*}, Olga Roman^{*}, Alanis Cordova^{*}, Amie Simmons^{*}, Xiao-Hong Sun^{*,†}, José Alberola-Ila^{*,†}

^{*}Arthritis and Clinical Immunology Program, Oklahoma Medical Research Foundation, Oklahoma City, OK 73104;

[†]Department of Cell Biology, University of Oklahoma Health Sciences Center, Oklahoma City, OK 73104

Abstract

Innate lymphoid cells (ILCs) are tissue-resident lymphoid cells that reside mostly at barrier surfaces and participate in the initial response against pathogens. They are classified into different types based on effector programs that are based on cytokine production and transcription factor expression. They all derive from the common lymphoid precursor, but the molecular mechanisms regulating ILC subset development is not well understood. Experiments using Id2 knockout mice have previously shown that E protein activity inhibition is an absolute requirement for the development of all ILC subsets. In this study, we use a genetic approach to demonstrate that small increases in E protein activity during ILC development selectively inhibit type 2 ILC development. Type 1 ILCs are mostly unperturbed, and type 3 ILC show only a minor inhibition. This effect is first evident at the ILC2 progenitor stage and is ILC intrinsic. Therefore, our results demonstrate that modulation of E protein activity can bias cell fate decisions in developing ILCs.

INTRODUCTION

The immune system initiates effective responses to multiple types of pathogens through different cell effector programs. Effector programs define cell responses that are primed toward the release of particular cytokines. The three most commonly described effector programs are type 1, releasing IFN- γ , type 2, releasing IL-5 and IL-13, and type 17, releasing IL-17. These effector programs were first described in CD4 Th cells and have recently been identified in other cell types, including innate immune cells such as invariant NKT (iNKT) cells and innate lymphoid cells (ILCs) (1, 2).

This article is distributed under the terms of the [CC BY-NC-ND 4.0 Unported license](https://creativecommons.org/licenses/by-nc-nd/4.0/).

Address correspondence and reprint requests to: Dr. José Alberola-Ila, Oklahoma Medical Research Foundation, 825 NE 13th Street, Oklahoma City, OK 73104. alberolaj@omrf.org.

The sequences presented in this article have been submitted to the Gene Expression Omnibus (<https://www.ncbi.nlm.nih.gov/geo>) under accession number GSE135195.

DISCLOSURES

The authors have no financial conflicts of interest.

ILCs are innate cells located mainly at barrier surfaces such as skin, gut, and lungs (3). They are activated by cytokines released by host cells because of barrier damage, and their responses differ based on their effector program. ILC responses are beneficial in many infections but can also cause detrimental effects. For example, type 2 ILCs (ILC2s) contribute to the immune response against *Nippostrongylus brasiliensis* (4–6) and *Strongyloides venezuelensis* (7) but are also one of the main producers of IL-5 and IL-13 in allergic asthma (8).

ILCs acquire effector programs during their development, which begins in the fetal liver in the embryo and later moves to the bone marrow. In the bone marrow, ILCs develop from the common lymphoid progenitor (CLP), which also gives rise to B cells and early thymic precursors. A subset of CLPs differentiates into common helper–like ILC precursors or common helper innate lymphoid progenitors (ChILPs). ILCs share this precursor with NK cells and lymphoid tissue inducer–like cells (9). The next stage of development, defined by upregulation of the transcription factor PLZF, is the ILC progenitor (ILCP). ILCPs give rise only to effector ILCs (10). These three cell types, type 1 ILCs (ILC1s), ILC2s, and type 3 ILCs (ILC3s), require the transcription factors TBET (10, 11), GATA3 (12), and ROR γ T (13), respectively, for their development, along with complex networks of other signaling molecules and transcription factors (14). However, how the differentiation decisions are initiated and reinforced in developing ILCs is still being elucidated.

Inhibitor of DNA-binding (ID) 2, a protein that inhibits the activity of E protein transcription factors, is essential for ILC development as ID2 knockout mice completely lack ILCs (15). E proteins are class I basic helix–loop–helix transcription factors. The members of the mammalian family of E proteins include HEB, E2–2, and two alternatively spliced proteins from the *E2A* gene, E12 and E47. E proteins have a dimerization domain and a DNA-binding domain. They homodimerize or heterodimerize with other E proteins or other members of the class II basic helix–loop–helix transcription factor family such as T cell acute lymphocytic leukemia 1 (TAL1) in hematopoietic cells. These dimers bind to sites in DNA called E boxes (sequence CANNTG) located in gene enhancer regions and affect transcription (16).

ID proteins are HLH proteins that lack DNA-binding domains. They heterodimerize with E proteins and function as dominant negative inhibitors of E protein activity by preventing E proteins from binding E boxes (17, 18). There are four mammalian ID proteins: ID1, ID2, ID3, and ID4, although only ID2 and ID3 are typically expressed in lymphoid cells (18). E protein activity functions on a gradient determined by the relative levels of E proteins and ID proteins, and different levels of activity have distinct effects on cell developmental decisions. Altering E protein activity along this gradient affects multiple developmental processes, including brain development and B cell commitment and differentiation (19, 20).

Although most research on ID protein and E protein function in ILC development has used knockout models that examine the extremes of the E protein activity gradient, we use a model that subtly increases E protein activity. Our cre-induced conditional knock-in mouse model expresses ET-2, a fusion protein between the transactivation domains of E47 and the dimerization domain of SCL/Tal1, which does not mediate homodimerization but has a high

affinity for E proteins (21, 22). ET-2 competes with ID proteins to bind to endogenous E proteins. ET-2 does not exhibit transcriptional activity by itself but acts as a transcriptional activator when associated with wild-type E47; therefore, overexpression of ET-2 decreases the effects of Id proteins and sustains E protein activity (23).

Using this model, our laboratories have previously established that small changes in E protein activity during NKT cell development affect effector program differentiation of NKTs, biasing them toward NKT2 and NKT17 development over NKT1 development (24). In this study, we have used the same ET-2 model, driven by Rag1-cre, to examine how sustained E protein activity affects ILC development. We found that sustained E protein activity in Rag1-cre;ET-2 mice profoundly inhibited ILC2 development, with the defect becoming apparent at the ILC2 progenitor (ILC2P) stage, whereas ILC1s were not affected, and ILC3s had only a minor defect. Therefore, our results show that E protein activity gradients play an important role in ILC subset differentiation and that ILC2s require the strongest E protein inhibition to proceed through development.

MATERIALS AND METHODS

Mice

All mice were maintained in a specific pathogen-free facility at Oklahoma Medical Research Foundation and were handled in compliance with guidelines established by the Institutional Animal Care and Use Committee. Generation of ROSA26-ET2 conditional knock-in was described previously (23). ROSA26-tdTomato reporter mice were obtained from The Jackson Laboratory (B6.Cg-*Gt(ROSA)26Sor^{tm9(CAG-tdTomato)Hze/J}* stock number 007909) (25). Rag1-Cre mice were obtained from Dr. Rabbitts (26). Mice were males and females used between 8 and 12 wk.

Preparation of cell suspensions

Bone marrow was isolated by gently crushing isolated femurs and tibias before filtration through 70- μ m filters and RBC lysis.

Lungs were perfused with 10 ml of PBS, diced, and incubated in 5 ml of medium containing 50 μ g/ml Liberase TH (124997; Roche) and 1 μ g/ml DNase I (E1011-A; Zymo Research) in a 37°C incubator for 45 min with shaking. In experiments in which CD27 was used as a surface marker, lungs were mechanically dissociated. Afterwards, cells were filtered through 70- μ m filters. In some experiments, cells were resuspended in 5 ml of 40% Percoll, overlaid with 5 ml of 60% Percoll, and centrifuged at 800 \times *g* for 20 min with no brake to collect the middle layer of lymphocytes.

Liver was perfused with 10 ml of PBS and mechanically dissociated through 70- μ m filters. Following dissociation, each liver was centrifuged at 400 \times *g* for 5 min, resuspended in 5 ml of 40% Percoll (Sigma-Aldrich), and then centrifuged at 800 \times *g* for 10 min. The supernatant was aspirated, and the cell pellet was resuspended in PBS containing 5% FCS.

To isolate interstitial epithelial lymphocytes (IEL) and lamina propria lymphocytes (LPL), the intestine was removed, cutting 0.5 cm below the stomach and 1 cm above the cecum.

The intestine was emptied of its contents and opened by making a lengthwise incision. Peyer patches were removed. The intestine was cut into 1-cm pieces, which were washed of excess mucous and then shaken at 37°C for 30 min in 25 ml of dithioerythritol solution (10% 10× HBBS, 10% 10× HEPES bicarbonate buffer, 10% FBS, with 1 mM EDTA [Honeywell Fluka]). The supernatant was removed, and the incubation was repeated. Supernatants from each incubation were combined and centrifuged at 1400 rpm for 5 min. Cell pellets were resuspended in 5 ml of 44% Percoll and underlaid with 5 ml of 67% Percoll and then centrifuged at 2000 rpm for 20 min without brake, yielding the IEL fraction. The IELs were washed with 30 ml of harvest medium (RPMI 1640 with 5% FBS, 2 mM HEPES, 1× penicillin/streptomycin (Pen/Strep), and 2 mM L-glutamine). The intestinal pieces were then subjected to two 30-min incubations at 37°C with shaking in 25 ml of EDTA solution (10% 10× HBBS, 2% 1M HEPES, 1× Pen/Strep, 2 mM L-glutamine, and 0.13 mM EDTA), discarding the supernatants. Intestinal pieces were washed with 30 ml of harvest medium for 5 min at 37°C with shaking and then digested for 45 min at 37°C with shaking using 30 ml of collagenase solution (RPMI 1640 containing 10% FBS, 2 mM HEPES, 2 mM L-glutamine, 1× Pen/Strep, 1 mM CaCl₂, 1 mM MgCl₂, and 100 mg/ml collagenase type 4). The digested tissue was passed through a 70-µm filter and centrifuged at 1400 rpm for 5 min. The cell pellet was resuspended in 8 ml of 44% Percoll and underlaid with 67% Percoll and then centrifuged at 2000 rpm for 20 min without brake, yielding the LPL fraction. The LPLs were washed with 30 ml of harvest medium.

Cytokine stimulation

Two to four million cells were resuspended in 1 ml of complete medium (RPMI containing 10% FBS, 1% L-glutamine, 1% Pen/Strep, 5% nonessential amino acids, 1% sodium pyruvate, 2% HEPES, and 0.1% 2-ME) in FACS tubes and incubated in a 37°C incubator with 5% CO₂ for 5 h with 500 ng/ml ionomycin, 30 ng/ml PMA, and 1 µl per sample of GolgiStop. After 5 h, cells were washed with PBS and stained for viability and surface markers. Cells were stained for cytokines using the BD Cytotfix/Cytoperm Kit.

For cytokine stimulation, ILCs were enriched by positive selection with anti-CD90.2 magnetic beads (Becton Dickinson) according to the manufacturer instructions and cultured in α-MEM (Life Technologies) supplemented with 20% FBS, Pen/Strep, 2-ME, and glutamine (Sigma), with 10 ng/ml each of IL-2, IL-7, IL-25, and IL-33 for 3 d. GolgiStop was added during the last 5 h of culture.

Flow cytometry

After cell suspensions were prepared, they were stained using LIVE/DEAD stains, either eBioscience Fixable Viability Dye eFluor 506 or BioLegend Zombie Aqua Fixable Viability Kit and then incubated with Fc block and then a biotinylated lineage mixture consisting of BD Lineage Cocktail from the bone marrow IMag Mouse Hematopoietic Progenitor (Stem) Cell Enrichment Set DM (catalog [Cat]: 558451) (Anti-mouse CD3e, clone 145-2C11, Anti-mouse CD11, clone M1/70, Anti-mouse CD45R/B220, clone RA3-6B2, Anti-mouse Ly-6G and Ly-6C [Gr-1], clone RB6-8C5, and anti-mouse TER-119/erythroid Cells, clone TER-119), supplemented with CD5 (BioLegend clone 53-7.3) followed by fluorochrome-conjugated Abs, including as follows: eBioscience: IL-13 PE (clone eBio13A), ST2 PE

(clone RMST2-2), EOMES eFluor 660 (clone Dan11mag), GATA3, PerCP-eFluor 710 (clone TWAJ), IL-13 PE-eFluor610 (clone eBio13A), B220 purified (clone RA3-6B2), CD11b purified (clone M1/70), CD11c bio (clone N418), CD127 PE (clone A7R34), $\alpha 4\beta 7$ PerCP-e710 (clone DATK32), and CD25 A700 (clone PC61.5); Becton Dickinson: IL-5 allophycocyanin (clone TRFK5), CD90-BV786 (clone 53-2.1), CD62L (L-selectin) PerCPCy5.5 (clone MEL-14), CD25 PECy7 (clone PC61), ROR γ_T BV421 (clone Q31-378), CD27 PECy7 (clone LG.3A10), CD19 purified (clone 1D3), CD3 bio (500A2), CD5 bio (53-7.3), TCR $\gamma\delta$ bio (clone GL3), and TCR $\gamma\delta$ PE (clone GL3); and BioLegend: SA-allophycocyanin, SA-allophycocyanin-Fire, CD90 allophycocyanin-Cy7 (clone 30-H12), IL-7R α (CD127) PE-Dazzle (clone A7R34), ST2 PE (clone DIH9) Flt3 Pe (clone A2F10), $\alpha 4\beta 7$ BV412 (clone DATK 32), IL-17A PerCpCy5.5 (clone TC11-18H10.1), T-bet PE/Dazzle594 (clone 4B10), FCeR1 bio (clone MAR-1), B220 bio (RA3-632), CD19 bio (6D5), CD11b bio (M1/70), Gr1 bio (RB6-865), NK1.1 bio (clone PK136), Ter-199 bio (clone Ter-119), CD8a bio (53-6.7), TCR β bio (H57-597), SA-PerCP-Cy5.5, CD45.2 Pacific Blue (clone 104), Sca-1 PECy7 (clone D7), cKit (CD117), allophycocyanin-Cy7 (clone 2B8), CD135 (Flt3), allophycocyanin (clone A2F10), ICOS (CD278), PECy7 (clone C398.4A), NK1.1 allophycocyanin-Cy7 (clone PK136), TCR β allophycocyanin (clone H57-597), Ter119 purified (clone TER-119), Gr1 purified (clone RB6-865), and TCR β purified (clone H57-597).

Intracellular staining was performed using the eBioscience Foxp3 Staining Buffer Kit.

OP9-DL1 cultures

Stocks of OP9-DL1 stromal cells were a gift from J. C. Zuñiga-Pflucker. All experiments were performed in MEM- α medium containing 20% FBS (Life Technologies), 1 \times Pen/Strep (Life Technologies), and 60 mM 2-ME (Sigma-Aldrich) and maintained in a 37°C incubator with 5% CO₂. Stromal cells were 70% confluent when lymphocytes were plated, at which point cultures were supplemented with murine IL-2, IL-7, and stem cell factor at 30 ng/ml each.

To purify CLPs, total bone marrow cells were isolated from mice and lysed in ACK RBC lysis buffer. All cells were stained with FCeR1, B220, CD19, Mac1, Gr1, CD11c, NK1.1, Ter-119, CD3, CD8a, CD5, TCR β , and TCR $\gamma\delta$ purified Abs in azide-free FACS buffer and then mixed with Rag IgG magnetic beads (QIAGEN) for lineage depletion. Lineage-negative cells were then sorted as CD45.2⁺Lin⁻CD127⁺Sca1^{int}c-kit^{int}Flt3⁺CD90.2⁻. One hundred sorted CLPs were plated in a single well on OP9-DL1 stromal cells. Medium was changed on day 4, and cells were replated onto fresh OP9-DL1 cells on days 7, 11, and 14. Cells were analyzed by flow cytometry on days 10, 14, and 17.

RNA sequencing

Bone marrow was taken from four to five pooled Rag1cre;ET-2 mice for each of four replicates. Cells from these combined mice were lineage depleted using the bone marrow IMag Mouse Hematopoietic Progenitor (Stem) Cell Enrichment Set DM (Cat: 558451) according to the manufacturer's instructions. The negative fraction was stained for ILC precursors, and GFP⁺ and GFP⁻ ILCP (Lin⁻ Flt3⁻ IL-7R α ⁺ $\alpha 4\beta 7$ ⁺ CD90⁺ CD25⁻) cells

were sorted using a FACS Aria into TRIzol. TRIzol samples were processed using Zymo Research kit RNA Clean & Concentrator (Cat: R1015S) Zymo Research kit Direct-zol RNA MicroPrep (Cat: R2060). An mRNA library was generated from extracted total RNA using the Trio RNA-Seq Kit from NuGEN Technologies. Briefly, extracted total RNA underwent DNase treatment followed by double-stranded cDNA generation. cDNA was first purified using Agencourt RNAClean XP beads and then further amplified using single primer isothermal amplification. Following end repair, adapter ligation, and amplification of properly ligated library molecules, the library underwent depletion of rRNA molecules using the NuGEN AnyDeplete system, a probe-based enzymatic digestion of unwanted molecules. Remaining library molecules were amplified again and quantified on an Invitrogen QuantSeq fluorometer followed by sizing on an Agilent TapeStation. After normalizing dilutions, the samples were pooled as equal volumes and sequenced on an Illumina NextSeq 500 with high output chemistry giving paired end 75-bp reads. Paired raw reads for each sample were trimmed from adapters using the Trimmomatic program (27).

The samples were decontaminated using bowtie2 (28). The reads were then aligned to the *Mus musculus* genome, GRCm38/mm1, using Kallisto (29). Aligned reads were annotated using the biomaRt “mmusculus_gene_ensembl” dataset in R. Genes with five or more zeros across samples were removed. Differential expression analysis was performed using the DESeq2 R package (30) to compare the ET-2 group to the normal littermate control (NLC) group. The criteria for differentially expressed transcripts were a fold change 1.5 and a false discovery rate p value <0.05 . The differentially expressed genes were then analyzed by the Ingenuity Pathway Analysis program.

The RNA sequencing (RNA-seq) data have been submitted to Gene Expression Omnibus (<https://www.ncbi.nlm.nih.gov/geo>) with accession number GSE135195.

Statistical analysis

All statistical analyses were performed using GraphPad Prism software. One-way ANOVA analyses were performed when comparing more than two populations. Two-tailed unpaired t tests were performed when comparing two populations. All error bars show SD.

RESULTS

Rag1-cre induces deletion in most ILCs

To test whether partially sustaining E protein activity during ILC development altered effector subset differentiation, we used a knock-in Rag1-cre (26) to induce ET-2 expression in CLPs as transcription from the Rag locus marks the earliest lymphocyte precursors in the bone marrow (31). Rag1-cre^{+/+} mice were bred to ET-2^{+/-} mice to generate Rag1-cre^{+/-}ET-2^{+/-} mice, hereafter referred to as ET-2 mice, and Rag1-cre^{+/-}ET-2^{-/-} mice, hereafter referred to as NLC mice. ET-2 mice have a floxed stop cassette followed by the ET-2 sequence, an IRES, and the GFP reporter gene in the ROSA-26 locus. To confirm that Rag1-cre-induced deletion of floxed alleles occurred in most ILCs, we bred Rag1-cre mice to ROSA26-tdTomato reporter mice (25), which have a floxed stop cassette before the tdTomato reporter gene and examined the expression of tdTomato in ILCs (defined as live

CD45⁺Lin⁻CD90⁺) in the bone marrow, lungs, and IEL and LPL of the intestine. As shown in Fig. 1A and 1B, most ILCs in all tissues examined were tdTomato⁺, confirming that Rag1-cre expression at the CLP stage is sufficient to delete a floxed allele in most developing ILCs. We also examined tdTomato expression at earlier stages of ILC differentiation in the bone marrow and observed that CLP and ChILP populations had a lower percentage of tdTomato⁺ cells than did ILC2Ps or ILC2Ps, which were comparable to mature ILCs (Supplemental Fig. 1). The earlier progenitors likely had fewer tdTomato⁺ cells because of a delay from the initial expression of tdTomato to our ability to detect the protein. Altogether, these results suggest that Rag1-cre is capable of inducing deletion in most ILC2Ps and can be used to induce ET-2 expression in developing ILCs.

ET-2-expressing ILCs are underrepresented in the bone marrow and lungs of Rag1-cre; ET-2 mice

We next analyzed ILC populations in ET-2 mice. Because the ET-2 knock-in model includes an IRES-GFP, we could track the fate of ILC precursors that express ET-2 (GFP⁺) versus their unaffected counterparts (GFP⁻) within the same mouse. We defined ILCs as live CD45⁺Lin⁻CD90⁺ and examined the percentage of GFP⁺ ILCs in bone marrow, lungs, and both the IEL and LPL of the intestine (Fig. 1C). As shown in Fig. 1D, ILCs in the intestinal IEL had a percentage of GFP⁺ cells similar to what was seen in Rag1-cre; tdTomato mice. However, ILCs from the bone marrow, lungs, and intestinal LPL had a lower percentage of GFP⁺ cells than did the ILCs from intestinal IEL, with the difference between bone marrow and IEL showing significance (Fig. 1D). Although Rag1-cre is expressed during the development of ILCs, not all precursors are positive for tdTomato⁺ in Rag1-cre;tdTomato mice, signifying that some early ILC precursors have the opportunity to escape ET-2 expression in ET-2 mice and develop into GFP⁻ ILCs. Therefore, expression of ET-2 (marked as GFP⁺) has a negative effect on the development of ILC populations in the bone marrow, lungs, and intestinal LPL, leading to an enrichment in ILCs that escaped recombination during development (GFP⁻). We reasoned that the difference in percentage of GFP⁺ cells among organs could be due to the different representation of ILC effector program subsets in those organs.

Expression of ET-2 is selectively detrimental for the development of ILC2s

As ILCs in the bone marrow, lungs, and intestinal LPL were enriched for cells that did not express ET-2, we investigated whether any ILC subsets were specifically affected by ET-2 expression during their development, focusing on the bone marrow and lungs as these organs showed the largest percentage of GFP⁻ ILCs. Although ILC effector program subsets are most specifically distinguished based on the expression of defining transcription factors, the permeabilization conditions required for nuclear transcription factor staining do not allow simultaneous detection of cytoplasmic GFP, and in our hands, the use of an Ab directed against GFP was not sufficient to separate a GFP⁺ population (data not shown). Therefore, for these experiments, we identified ILC subsets using a surface marker staining profile that we verified with transcription factor expression (Supplemental Fig. 2a-c). We define ILCs as live CD45⁺Lin⁻CD90⁺IL-7R α ⁺CD62L⁻. Gating on CD62L⁻ eliminates most NK cells from the analysis (Supplemental Fig. 2d) and makes identification of ILC1s easier. Within this ILC gate, we defined ILC1s as CD27⁺ST2⁻, ILC2s as ST2⁺CD27^{int}, and ILC3s as

CD27⁻ST2⁻ (Fig. 2A). The majority of cells in our defined populations of ILC2s and NK cells are positive for their effector program's transcription factor (Supplemental Fig. 2b, 2d). However, CD27⁻ST2⁻ ILCs are only 48.6 ± 6.8% RORγt⁺ in the bone marrow and 48.17 ± 14.81% RORγt⁺ in the lungs (Supplemental Fig. 2e), meaning that CD27⁻ST2⁻ ILCs contain the ILC3 population but are not exclusively ILC3s. NKp46 and CCR6 have been used to classify ILC3s in small intestine preparations, but it has been shown that most ILC3s in the lung are NKp46⁻, and only 20% are CCR6⁺ (32). We confirmed these results while trying to optimize our surface staining approach. Another recent paper used CD4 expression to identify ILC3 in lymph nodes, but we were not able to reproduce this staining (33). Similarly, CD27⁺ST2⁻ ILCs contain the majority of TBET⁺ cells, but not all of these cells are TBET⁺ (Supplemental Fig. 2a).

We first compared ILC populations and ILC subset populations between NLC mice and ET-2 mice and found no significant differences (Fig. 2B, 2C). If ET-2 expression affects the development of a population of cells, a different ratio of GFP⁺ to GFP⁻ cells would be observed as compared with other populations, with a lower percentage of GFP⁺ cells indicating a negative effect of sustained E protein activity. When we quantified GFP expression within ILC effector program populations, we observed that ILC2s, but not ILC1s and ILC3s, had a significantly lower percentage of GFP⁺ cells in both the bone marrow and lungs (Fig. 2D, 2E). This indicates that sustained E protein activity during ILC development has a negative effect on ILC2 development, whereas ILC1 and ILC3 development are not affected when defining these populations based on their surface markers.

ILC effector programs can also be identified by the cytokines they produce. To confirm and extend our analysis, we defined ILC subsets in Rag-1-cre;ET-2 mice functionally, based on their ability to secrete the cytokines of their effector program when stimulated. We stimulated total bone marrow and lung cells with PMA (30 ng/ml) and ionomycin (500 ng/ml) for 5 h in the presence of monensin and analyzed cytokine expression in ILCs, defined as live CD45⁺Lin⁻CD90⁺IL-7Rα⁺. In these experiments, we defined ILC1s as IFN-γ-producing cells, ILC2s as IL-5- and IL-13-producing cells, and ILC3s as IL-17-producing cells (Fig. 3A). Subset representation was not different between NLC and ET-2 mice, but when we examined the GFP expression within each population of ILCs in ET-2 mice, we observed a dramatic underrepresentation of GFP⁺ cells within the ILC2 population in both the bone marrow and lungs (Fig. 3B, 3C), confirming our previous results with surface markers. Additionally, we observed a slight underrepresentation of GFP⁺ cells within the ILC3 population in the bone marrow (Fig. 3B). Therefore, sustained E protein activity by ET-2 has a strong negative effect on ILC2s, a mild effect on ILC3s, and no effect on ILC1s when defining these populations based on their produced cytokines.

NK cells did not show a population defect between NLC and ET-2 mice. In fact, when comparing the percentage of NK cells within the CD45⁺ population between NLC and ET-2 mice, NK cells showed a population increase in the bone marrow (Supplemental Fig. 3a), although they showed no difference in the lungs (Supplemental Fig. 3b). NK cells showed an increase in the percentage of GFP⁺ cells as compared with ILCs in the bone marrow and no difference in the percentage of GFP⁺ cells in the lungs (Supplemental Fig. 3c, 3d).

Therefore, sustained E protein activity does not negatively affect NK cell development and may, in fact, promote the development of these cells in the bone marrow.

ET-2 expression inhibits ILC2 differentiation at the ILC2P stage in the bone marrow

To determine at which stage of ILC2 development sustained E protein activity begins to have a negative effect, we examined ILCPs in the bone marrow, beginning with the CLP. As ILCs develop from CLPs, they downregulate Flt3 and upregulate $\alpha 4\beta 7$ (9). These cells are a heterogeneous population called α LPs and include ChILPs (9), ILCPs (10), and an ILC2-specific progenitor termed ILC2P (12). CD90 is upregulated as cells develop from ChILPs to ILCPs, and CD25 marks ILC2Ps (Fig. 4A).

We observed no significant difference in population frequencies or cell numbers of CLPs, ChILPs, ILCPs, or ILC2Ps between ET-2 mice and NLC mice (Fig. 4B). However, when we analyzed the percentage of GFP⁺ cells within these populations, we saw that they were slowly increasing until the ILC2P stage, where they sharply decreased (Fig. 4C). Therefore, ET-2 expression selectively inhibits ILC2 differentiation, starting at the ILC2P stage.

ET-2 expression inhibits development of in vitro ILC2s cultured from sorted CLPs

Many factors could potentially contribute to ILC development in vivo, including the local cytokine environment and interactions with other cells. These factors could influence ILC development in ET-2 mice. For example, ET-2 mice contain abundant ET-2-expressing T and B cells, which could exert an indirect effect on ILC development. To determine if the effect of sustained E protein activity on ILC2 development was cell intrinsic, we used an in vitro system to look at ILC2 development from CLPs. We sorted CLPs from lineage-depleted bone marrow from ET-2 mice and NLCs, plated them over a layer of OP9-DL1 stromal cells, and cultured them for up to 17 d in medium that contained stem cell factor, IL-2, and IL-7. ILC2 development was analyzed by flow cytometry at days 10, 14, and 17. Cultures grew well and increased from the original 100 cells plated per well to a total of $3.318 \times 10^5 \pm 0.761 \times 10^5$ cells by day 17, with no significant difference in cell numbers between NLC and ET-2 mice (data not shown). We defined ILC2s as live CD45⁺TCR β ⁻TCR $\gamma\delta$ ⁻CD25⁺ICOS⁺ $\alpha 4\beta 7$ ⁻, and we examined the percentage of GFP⁺ cells within the ILC2 gate and the live CD45⁺ gate (Fig. 5A). Overall, the percentage of ILC2s out of all live CD45⁺TCR β ⁻TCR $\gamma\delta$ ⁻ cells was not significantly different on any days (Fig. 5B). However, the percentage of GFP⁺ ILC2s was lower than the percentage of GFP⁺ CD45⁺TCR⁻ cells, showing significance on days 10 and 14 (Fig. 5C). From these data, we conclude that sustained E protein activity negatively affects ILC2 development in vitro, and ET-2 has an effect on ILC2 development outside the context of the bone marrow environment, suggesting that this effect is cell intrinsic.

ET-2 expression results in small expression changes of several genes involved in ILC2 and ILC3 development

To determine which genes are affected by sustained E protein activity in ILCs, we performed RNA-seq on sorted GFP⁺ and GFP⁻ ILCs (live Lin⁻Flt3⁻IL-7R α ⁺ $\alpha 4\beta 7$ ⁺CD90⁺CD25⁻) from ET-2 and NLC bone marrow. Analyzing results with DESeq2, we found 99 differentially expressed genes (fold change ≥ 1.5 and a false discovery rate p

value <0.05) between GFP⁺ ET-2 ILCs and NLC ILCs, with 36 genes downregulated in ET-2 ILCs and 63 upregulated in ET-2 ILCs (Supplemental Table I). None of these genes are obvious candidates to inhibit ILC2 development, and ingenuity pathway analysis of the differentially expressed genes was not very revealing. We then compared the expression of genes previously identified as important for ILC subset development (34, 35) and observed that whereas many genes essential for the development of all ILCs or specific for ILC1 were expressed at similar levels in GFP⁺ and GFP⁻ ILCs, some genes specific for ILC2 (ROR α , IL-17R α , GATA-3, and ICOS) or ILC3 (Ahr, ROR γ , and Runx3) development were slightly underexpressed in ET-2-expressing ILCs (Fig. 6). Although it is currently unclear if any of these genes are direct targets of E protein activity in ILC precursors, these results suggest that whereas slightly raising E protein activity does not result in a major shift in gene expression, the cumulative effect of these small changes has a profound effect and make ET-2-expressing ILCs less fit to develop into ILC2s and, less dramatically, ILC3s.

ET-2 expression negatively affects ILC2 function

Although sustained E protein activity has a negative effect on ILC2 development in ET-2 mice, a number of GFP⁺ ILC2 cells still develop. Therefore, we tested whether sustained E protein activity in these cells affected their function. ILCs accomplish their functions through the release of cytokines. For ILC2s, these cytokines are IL-5 and IL-13. We noticed in our previous results that the percentage of GFP⁺ ILC2s was similar when defining these cells as ST2⁺ or as IL-5- and IL-13-producing ILCs. This similar percentage of GFP⁺ cells hinted that ST2⁺ ILC2s are also cytokine-producing ILC2s, but we wanted to directly compare cytokine production in GFP⁻ and GFP⁺ ILC2s. To do this, we stimulated bone marrow and lung using PMA (30 ng/ml) and ionomycin (500 ng/ml) with monensin for 5 h and examined the production of IL-5 and IL-13 within both GFP⁻ and GFP⁺ ILC2s, defined as live CD45⁺Lin⁻CD90⁺ST2⁺ cells (Fig. 7A). GFP⁺ ILC2s showed a significant decrease in the percentage of cytokine-producing cells (defined as producing IL-5 alone, IL-13 alone, or IL-5 and IL-13 together) in the bone marrow (Fig. 7B). However, GFP⁻ and GFP⁺ ILC2s in the lungs showed no significant difference in cytokine production. To extend our results to a more physiological stimulus, we determined cytokine production after culture with 10 ng/ml each of IL-2, IL-7, IL-25, and IL-33 for 72 h. Under these conditions, we observed a small but significant decrease in cytokine production by ET-2-expressing ILC2s (Fig. 7C). These results suggest that sustained E protein activity does have an effect on ILC2 function once these cells have developed, at least in the bone marrow.

DISCUSSION

Inhibition of E protein activity is required for ILC development, as illustrated by the lack of ILCs in ID2 knockout mice (15). However, our results show for the first time that the degree of E protein activity inhibition has a selective effect on different ILC effector program subsets. Using ET-2 mice to sustain E protein activity during ILC development showed a negative effect on ILC2 development, with a mild effect on ILC3s and no effect on ILC1s. This is in contrast to our previous work using the ET-2 model to sustain E protein activity during iNKT cell development using CD4-cre;ET-2 mice, which biased cells toward NKT2 and NKT17 effector subset development at the expense of the NKT1 subset (24). This

dissimilarity suggests that although the different effector programs have many common regulatory networks (36–39), some of the molecular switches differ among lineages.

Different genetic approaches to changing E protein activity have unique effects on lineage differentiation and effector program decisions in iNKT cells (24, 40, 41) and in $\gamma\delta$ T cells (42–45). We were therefore not surprised to find that the subtle increase in E protein activity induced by ET-2 expression during ILC development caused a different effect to that observed in experiments in which ID2 was deleted, resulting in unrestrained E protein activity (4, 46). ID2 knockout mice demonstrated that inhibition of E protein activity is essential for the development of all ILCs. In contrast, our data show that whereas ILC1s and ILC3s can develop in the presence of a higher level of E protein activity, ILC2s have a more stringent requirement for E protein activity inhibition during development. Interestingly, in the thymus of ID1 transgenic mice, where E protein activity is inhibited more severely than normal, a population of thymic-derived ILC2s increases dramatically (47). A similar phenotype was seen in the thymus of mice that have the two E proteins E2A and HEB knocked out or that had inducible ID2 expression (47–49).

Altogether, our results suggest that a small increase in E protein activity affects ILC effector subsets differently, with ILC1s unaffected, ILC3s slightly affected, and ILC2 strongly negatively affected. Because ET-2 is expressed in all cells that have expressed Rag, and the bone marrow has abundant populations of B and T cells, it was formally possible that the inhibitory effect observed on the ILC2 could be due to alterations in these other cells. Although unlikely, because GFP⁻ ILC2s develop normally, we performed in vitro experiments on sorted CLPs under conditions that favor ILC2 development. These experiments recapitulated the results of our in vivo data, supporting that the effect of sustained E protein activity on ILC2 development is cell intrinsic.

We were surprised that the defect in ILC2 development was only observable when looking at the percentage of GFP⁺ cells within that population, indicating that developing GFP⁻ ILCs compensate for the negative effect ET-2 has on ILC2 development. The GFP⁻ minority of ILC precursors at earlier developmental stages became the majority of cells by the ILC2P stage. Whether this compensation is driven by increased proliferation or survival of these precursors, these results imply some undetermined population-sensing mechanism within this ILC subset.

ILC2s were clearly the most sensitive subset to small increases in E protein activity, with a clear selection against precursors that expressed ET-2. However, whereas we were not able to observe any effect on ILC1 development, the effect on ILC3 was intermediate. We did not observe an effect of ET-2 on ILC3 development when ILC3s were defined as CD27⁻ST2⁻ ILCs, but we observed a small but significant decrease in the percentage of ET-2-expressing ILC3s when defined functionally as IL-17-producing cells. This discrepancy is probably because of the fact that CD27⁻ST2⁻ ILCs are only $48.6 \pm 6.798\%$ ROR γ t⁺ in the bone marrow and $48.17 \pm 14.81\%$ ROR γ t⁺ in the lungs (Supplemental Fig. 3e), leaving more than half the cells, which may not be ILC3s and may not be affected by ET-2 expression. An alternative explanation could be that ILC3s develop normally in the presence of ET-2 but are functionally defective, and, therefore, fewer IL-17-producing ILC3s are GFP⁺.

Our results show that sustained E protein activity during ILC2 development negatively affects the ability of these cells to produce their effector program-defining cytokines. However, we do not know if this is because of a problem during development or to an effect of ET-2 on mature ILC2s. To interrogate this, we would need to use an inducible *cre* to begin sustaining E protein activity after ILC2s have already developed.

There is currently no direct evidence that E protein activity levels are correlated with effector program development cell fate decisions in ILCs, but our data predict that ILC2 development would be favored in ILCPs with high expression of ID2 compared with other ILCPs with lower ID2 expression levels. Not much is known about the signals that regulate ID2 early in ILC lineage development, although it is thought to be downstream of Nfil3, which is itself regulated by IL-7 in CLPs (50). To our knowledge, a possible correlation between ID2 expression levels and commitment to a certain ILC subset has not been tested. The mechanism behind the selective effect of increased E protein activity on ILC2 development is partially answered in our RNA-seq data, which showed lower expression of many ILC2-associated genes in ET-2-expressing ILCPs, but other factors may be involved as well. Runx3 is a transcription factor that is essential for ILC1 development and is a positive regulator of ILC3 differentiation while having no effect on ILC2 development (51). We found Runx3 to be slightly less expressed in ILCPs from ET-2 mice than in ILCPs from NLCs. Changes in Runx3 expression or activity have been shown to affect ID2 expression in mesenchymal stem cells (52). It is possible that Runx3 in ILC1 and ILC3s might play a role in counteracting the effect of sustained E protein activity during ILC development in ET-2 mice, although further experiments are required to test this hypothesis.

Although Th cells become primed toward an effector program during peripheral activation, influenced by the APCs and cytokine milieu surrounding them, innate immune cells like NKT cells and ILCs acquire effector programs during their development and therefore are able to initiate an early response to invading pathogens and contribute to the cytokine environment that will later influence CD4 Th cell differentiation. However, these effector programs are not static (53), and recent data suggest that their plasticity can be influenced by multiple factors, including cytokines such as IL-2, IL-23, IL-1 β , IL-12, and IL-18 and cells such as CD14⁺ or CD14⁻ dendritic cells (54–56). Therefore, understanding how ILC effector programs develop could lead to new insights and drug targets to harness this plasticity and shift ILCs away from pathogenic effector programs and toward beneficial ones, such as shifting cells away from an ILC2 fate in asthma patients. Our experiments in this study suggest that alterations in E protein activity could play a role in this process.

Supplementary Material

Refer to Web version on PubMed Central for supplementary material.

ACKNOWLEDGMENTS

We thank Dr. S. Kovats for critical discussion of the results. We also thank the Oklahoma Medical Research Institute Flow Cytometry Core for cell sorting, the Next Generation Sequencing and Quantitative Analysis Cores for RNA-seq and analysis, and the Comparative Medicine department for animal husbandry.

This work was supported by National Institutes of Health funding to J.A.-I. (AI122693). H.B. was partially supported by an Oklahoma Medical Research Foundation Capra predoctoral fellowship and an American Association of Immunologists predoctoral fellowship.

Abbreviations used in this article:

Cat	catalog
ChILP	common helper innate lymphoid progenitor
CLP	common lymphoid progenitor
ID	inhibitor of DNA-binding
IEL	interstitial epithelial lymphocyte
ILC	innate lymphoid cell
ILC1	type 1 ILC
ILC2	type 2 ILC
ILC3	type 3 ILC
ILCP	ILC progenitor
ILC2P	ILC2 progenitor
iNKT	invariant NKT
LPL	lamina propria lymphocyte
NLC	normal littermate control
Pen/Strep	penicillin/streptomycin
RNA-seq	RNA sequencing

REFERENCES

1. Constantinides MG, and Bendelac A. 2013 Transcriptional regulation of the NKT cell lineage. *Curr. Opin. Immunol* 25: 161–167. [PubMed: 23402834]
2. Robinette ML, and Colonna M. 2016 Immune modules shared by innate lymphoid cells and T cells. *J. Allergy Clin. Immunol* 138: 1243–1251. [PubMed: 27817796]
3. Gasteiger G, Fan X, Dikiy S, Lee SY, and Rudensky AY. 2015 Tissue residency of innate lymphoid cells in lymphoid and non-lymphoid organs. *Science* 350: 981–985. [PubMed: 26472762]
4. Moro K, Yamada T, Tanabe M, Takeuchi T, Ikawa T, Kawamoto H, Furusawa J, Ohtani M, Fujii H, and Koyasu S. 2010 Innate production of T(H)2 cytokines by adipose tissue-associated c-Kit(+)/Sca-1(+) lymphoid cells. *Nature* 463: 540–544. [PubMed: 20023630]
5. Neill DR, Wong SH, Bellosi A, Flynn RJ, Daly M, Langford TK, Bucks C, Kane CM, Fallon PG, Pannell R, et al. 2010 Nuocytes represent a new innate effector leukocyte that mediates type-2 immunity. *Nature* 464: 1367–1370. [PubMed: 20200518]
6. Price AE, Liang HE, Sullivan BM, Reinhardt RL, Eisley CJ, Erle DJ, and Locksley RM. 2010 Systemically dispersed innate IL-13-expressing cells in type 2 immunity. *Proc. Natl. Acad. Sci. USA* 107: 11489–11494. [PubMed: 20534524]

7. Yasuda K, Muto T, Kawagoe T, Matsumoto M, Sasaki Y, Matsushita K, Taki Y, Futatsugi-Yumikura S, Tsutsui H, Ishii KJ, et al. 2012 Contribution of IL-33-activated type II innate lymphoid cells to pulmonary eosinophilia in intestinal nematode-infected mice. *Proc. Natl. Acad. Sci. USA* 109: 3451–3456. [PubMed: 22331917]
8. Klein Wolterink RG, Kleinjan A, van Nimwegen M, Bergen I, de Bruijn M, Levani Y, and Hendriks RW. 2012 Pulmonary innate lymphoid cells are major producers of IL-5 and IL-13 in murine models of allergic asthma. *Eur. J. Immunol* 42: 1106–1116. [PubMed: 22539286]
9. Klose CSN, Flach M, Möhle L, Rogell L, Hoyler T, Ebert K, Fabiunke C, Pfeifer D, Sexl V, Fonseca-Pereira D, et al. 2014 Differentiation of type 1 ILCs from a common progenitor to all helper-like innate lymphoid cell lineages. *Cell* 157: 340–356. [PubMed: 24725403]
10. Constantinides MG, McDonald BD, Verhoef PA, and Bendelac A. 2014 A committed precursor to innate lymphoid cells. *Nature* 508: 397–401. [PubMed: 24509713]
11. Daussy C, Faure F, Mayol K, Viel S, Gasteiger G, Charrier E, Bienvenu J, Henry T, Debien E, Hasan UA, et al. 2014 T-bet and Eomes instruct the development of two distinct natural killer cell lineages in the liver and in the bone marrow. *J. Exp. Med* 211: 563–577. [PubMed: 24516120]
12. Hoyler T, Klose CS, Souabni A, Turqueti-Neves A, Pfeifer D, Rawlins EL, Voehringer D, Busslinger M, and Diefenbach A. 2012 The transcription factor GATA-3 controls cell fate and maintenance of type 2 innate lymphoid cells. *Immunity* 37: 634–648. [PubMed: 23063333]
13. Sawa S, Cherrier M, Lochner M, Satoh-Takayama N, Fehling HJ, Langa F, Di Santo JP, and Eberl G. 2010 Lineage relationship analysis of ROR γ mat+ innate lymphoid cells. *Science* 330: 665–669. [PubMed: 20929731]
14. Zhong C, and Zhu J. 2017 Transcriptional regulators dictate innate lymphoid cell fates. *Protein Cell* 8: 242–254. [PubMed: 28108952]
15. Yagi R, Zhong C, Northrup DL, Yu F, Bouladoux N, Spencer S, Hu G, Barron L, Sharma S, Nakayama T, et al. 2014 The transcription factor GATA3 is critical for the development of all IL-7R α -expressing innate lymphoid cells. *Immunity* 40: 378–388. [PubMed: 24631153]
16. Massari ME, and Murre C. 2000 Helix-loop-helix proteins: regulators of transcription in eucaryotic organisms. *Mol. Cell. Biol* 20: 429–440. [PubMed: 10611221]
17. Engel I, and Murre C. 2001 The function of E- and Id proteins in lymphocyte development. *Nat. Rev. Immunol* 1: 193–199. [PubMed: 11905828]
18. Kee BL 2009 E and ID proteins branch out. *Nat. Rev. Immunol* 9: 175–184. [PubMed: 19240756]
19. Ravanpay AC, and Olson JM. 2008 E protein dosage influences brain development more than family member identity. *J. Neurosci. Res* 86: 1472–1481. [PubMed: 18214987]
20. Zhuang Y, Cheng P, and Weintraub H. 1996 B-lymphocyte development is regulated by the combined dosage of three basic helix-loop-helix genes, E2A, E2–2, and HEB. *Mol. Cell. Biol* 16: 2898–2905. [PubMed: 8649400]
21. Park ST, and Sun XH. 1998 The Tal1 oncoprotein inhibits E47-mediated transcription. Mechanism of inhibition. *J. Biol. Chem* 273: 7030–7037. [PubMed: 9507011]
22. Park ST, Nolan GP, and Sun XH. 1999 Growth inhibition and apoptosis due to restoration of E2A activity in T cell acute lymphoblastic leukemia cells. *J. Exp. Med* 189: 501–508. [PubMed: 9927512]
23. Cochrane SW, Zhao Y, Welner RS, and Sun XH. 2009 Balance between Id and E proteins regulates myeloid-versus-lymphoid lineage decisions. *Blood* 113: 1016–1026. [PubMed: 18927439]
24. Hu T, Wang H, Simmons A, Bazaña S, Zhao Y, Kovats S, Sun XH, and Alberola-Ila J. 2013 Increased level of E protein activity during invariant NKT development promotes differentiation of invariant NKT2 and invariant NKT17 subsets. *J. Immunol* 191: 5065–5073. [PubMed: 24123679]
25. Madisen L, Zwingman TA, Sunkin SM, Oh SW, Zariwala HA, Gu H, Ng LL, Palmiter RD, Hawrylycz MJ, Jones AR, et al. 2010 A robust and high-throughput Cre reporting and characterization system for the whole mouse brain. *Nat. Neurosci* 13: 133–140. [PubMed: 20023653]
26. McCormack MP, Forster A, Drynan L, Pannell R, and Rabbitts TH. 2003 The LMO2 T-cell oncogene is activated via chromosomal translocations or retroviral insertion during gene therapy but has no mandatory role in normal T-cell development. *Mol. Cell. Biol* 23: 9003–9013. [PubMed: 14645513]

27. Bolger AM, Lohse M, and Usadel B. 2014 Trimmomatic: a flexible trimmer for Illumina sequence data. *Bioinformatics* 30: 2114–2120. [PubMed: 24695404]
28. Langmead B, and Salzberg SL. 2012 Fast gapped-read alignment with Bowtie 2. *Nat. Methods* 9: 357–359. [PubMed: 22388286]
29. Bray NL, Pimentel H, Melsted P, and Pachter L. 2016 Near-optimal probabilistic RNA-seq quantification. [Published erratum appears in 2016 *Nat. Biotechnol.* 34: 888.] *Nat. Biotechnol* 34: 525–527. [PubMed: 27043002]
30. Love MI, Huber W, and Anders S. 2014 Moderated estimation of fold change and dispersion for RNA-seq data with DESeq2. *Genome Biol.* 15: 550. [PubMed: 25516281]
31. Igarashi H, Gregory SC, Yokota T, Sakaguchi N, and Kincade PW. 2002 Transcription from the RAG1 locus marks the earliest lymphocyte progenitors in bone marrow. *Immunity* 17: 117–130. [PubMed: 12196284]
32. Dutton EE, Camelo A, Sleeman M, Herbst R, Carlesso G, Belz GT, and Withers DR. 2017 Characterisation of innate lymphoid cell populations at different sites in mice with defective T cell immunity. *Wellcome Open Res.* 2: 117. [PubMed: 29588921]
33. Dutton EE, Gajdasik DW, Willis C, Fiancette R, Bishop EL, Camelo A, Sleeman MA, Coccia M, Didierlaurent AM, Tomura M, et al. 2019 Peripheral lymph nodes contain migratory and resident innate lymphoid cell populations. *Sci. Immunol* 4: eaau8082. [PubMed: 31152090]
34. Robinette ML, Fuchs A, Cortez VS, Lee JS, Wang Y, Durum SK, Gilfillan S, and Colonna M, Immunological Genome Consortium. 2015 Transcriptional programs define molecular characteristics of innate lymphoid cell classes and subsets. *Nat. Immunol* 16: 306–317. [PubMed: 25621825]
35. Yu Y, Tsang JC, Wang C, Clare S, Wang J, Chen X, Brandt C, Kane L, Campos LS, Lu L, et al. 2016 Single-cell RNA-seq identifies a PD-1^{hi} ILC progenitor and defines its development pathway. *Nature* 539: 102–106. [PubMed: 27749818]
36. Fang D, and Zhu J. 2017 Dynamic balance between master transcription factors determines the fates and functions of CD4 T cell and innate lymphoid cell subsets. *J. Exp. Med* 214: 1861–1876. [PubMed: 28630089]
37. Koues OI, Collins PL, Cella M, Robinette ML, Porter SI, Pyfrom SC, Payton JE, Colonna M, and Oltz EM. 2016 Distinct gene regulatory pathways for human innate versus adaptive lymphoid cells. *Cell* 165: 1134–1146. [PubMed: 27156452]
38. Shih HY, Sciumè G, Poholek AC, Vahedi G, Hirahara K, Villarino AV, Bonelli M, Bosselut R, Kanno Y, Muljo SA, and O’Shea JJ. 2014 Transcriptional and epigenetic networks of helper T and innate lymphoid cells. *Immunol. Rev* 261: 23–49. [PubMed: 25123275]
39. Shih HY, Sciumè G, Mikami Y, Guo L, Sun HW, Brooks SR, Urban JF Jr., Davis FP, Kanno Y, and O’Shea JJ. 2016 Developmental acquisition of regulomes underlies innate lymphoid cell functionality. *Cell* 165: 1120–1133. [PubMed: 27156451]
40. D’Cruz LM, Stradner MH, Yang CY, and Goldrath AW. 2014 E and Id proteins influence invariant NKT cell sublineage differentiation and proliferation. *J. Immunol* 192: 2227–2236. [PubMed: 24470501]
41. Verykokakis M, Krishnamoorthy V, Iavarone A, Lasorella A, Sigvardsson M, and Kee BL. 2013 Essential functions for ID proteins at multiple checkpoints in invariant NKT cell development. *J. Immunol* 191: 5973–5983. [PubMed: 24244015]
42. Lauritsen JP, Wong GW, Lee SY, Lefebvre JM, Ciofani M, Rhodes M, Kappes DJ, Zúñiga-Pflücker JC, and Wiest DL. 2009 Marked induction of the helix-loop-helix protein Id3 promotes the gammadelta T cell fate and renders their functional maturation Notch independent. *Immunity* 31: 565–575. [PubMed: 19833086]
43. Ueda-Hayakawa I, Mahlios J, and Zhuang Y. 2009 Id3 restricts the developmental potential of gamma delta lineage during thymopoiesis. *J. Immunol* 182: 5306–5316. [PubMed: 19380777]
44. Verykokakis M, Boos MD, Bendelac A, Adams EJ, Pereira P, and Kee BL. 2010 Inhibitor of DNA binding 3 limits development of murine slam-associated adaptor protein-dependent “innate” gammadelta T cells. *PLoS One* 5: e9303. [PubMed: 20174563]

45. Zhang B, Lin YY, Dai M, and Zhuang Y. 2014 Id3 and Id2 act as a dual safety mechanism in regulating the development and population size of innate-like $\gamma\delta$ T cells. *J. Immunol* 192: 1055–1063. [PubMed: 24379125]
46. Yokota Y, Mansouri A, Mori S, Sugawara S, Adachi S, Nishikawa S, and Gruss P. 1999 Development of peripheral lymphoid organs and natural killer cells depends on the helix-loop-helix inhibitor Id2. *Nature* 397: 702–706. [PubMed: 10067894]
47. Wang HC, Qian L, Zhao Y, Mengarelli J, Adrianto I, Montgomery CG, Urban JF Jr., Fung KM, and Sun. XH 2017 Downregulation of E protein activity augments an ILC2 differentiation program in the thymus. *J. Immunol* 198: 3149–3156. [PubMed: 28258196]
48. Miyazaki M, Miyazaki K, Chen K, Jin Y, Turner J, Moore AJ, Saito R, Yoshida K, Ogawa S, Rodewald HR, et al. 2017 The E-Id protein axis specifies adaptive lymphoid cell identity and suppresses thymic innate lymphoid cell development. *Immunity* 46: 818–834.e4. [PubMed: 28514688]
49. Qian L, Bajana S, Georgescu C, Peng V, Wang HC, Adrianto I, Colonna M, Alberola-Ila J, Wren JD, and Sun XH. 2019 Suppression of ILC2 differentiation from committed T cell precursors by E protein transcription factors. *J. Exp. Med* 216: 884–899. [PubMed: 30898894]
50. Xu W, Domingues RG, Fonseca-Pereira D, Ferreira M, Ribeiro H, Lopez-Lastra S, Motomura Y, Moreira-Santos L, Bihl F, Braud V, et al. 2015 NFIL3 orchestrates the emergence of common helper innate lymphoid cell precursors. *Cell Rep.* 10: 2043–2054. [PubMed: 25801035]
51. Ebihara T, Song C, Ryu SH, Plougastel-Douglas B, Yang L, Levanon D, Groner Y, Bern MD, Stappenbeck TS, Colonna M, et al. 2015 Runx3 specifies lineage commitment of innate lymphoid cells. *Nat. Immunol* 16: 1124–1133. [PubMed: 26414766]
52. Wang Y, Feng Q, Ji C, Liu X, Li L, and Luo J. 2017 RUNX3 plays an important role in mediating the BMP9-induced osteogenic differentiation of mesenchymal stem cells. *Int. J. Mol. Med* 40: 1991–1999. [PubMed: 29039519]
53. Colonna M 2018 Innate lymphoid cells: diversity, plasticity, and unique functions in immunity. *Immunity* 48: 1104–1117. [PubMed: 29924976]
54. Bernink JH, Krabbendam L, Germar K, de Jong E, Gronke K, Kofoed-Nielsen M, Munneke JM, Hazenberg MD, Villaudy J, Buskens CJ, et al. 2015 Interleukin-12 and -23 control plasticity of CD127(+) group 1 and group 3 innate lymphoid cells in the intestinal lamina propria. *Immunity* 43: 146–160. [PubMed: 26187413]
55. Ohne Y, Silver JS, Thompson-Snipes L, Collet MA, Blanck JP, Cantarel BL, Copenhaver AM, Humbles AA, and Liu YJ. 2016 IL-1 is a critical regulator of group 2 innate lymphoid cell function and plasticity. [Published erratum appears in 2016 *Nat. Immunol.* 17: 1005.] *Nat. Immunol* 17: 646–655. [PubMed: 27111142]
56. Silver JS, Kearley J, Copenhaver AM, Sanden C, Mori M, Yu L, Pritchard GH, Berlin AA, Hunter CA, Bowler R, et al. 2016 Inflammatory triggers associated with exacerbations of COPD orchestrate plasticity of group 2 innate lymphoid cells in the lungs. [Published erratum appears in 2016 *Nat. Immunol.* 17: 1005.] *Nat. Immunol* 17: 626–635. [PubMed: 27111143]

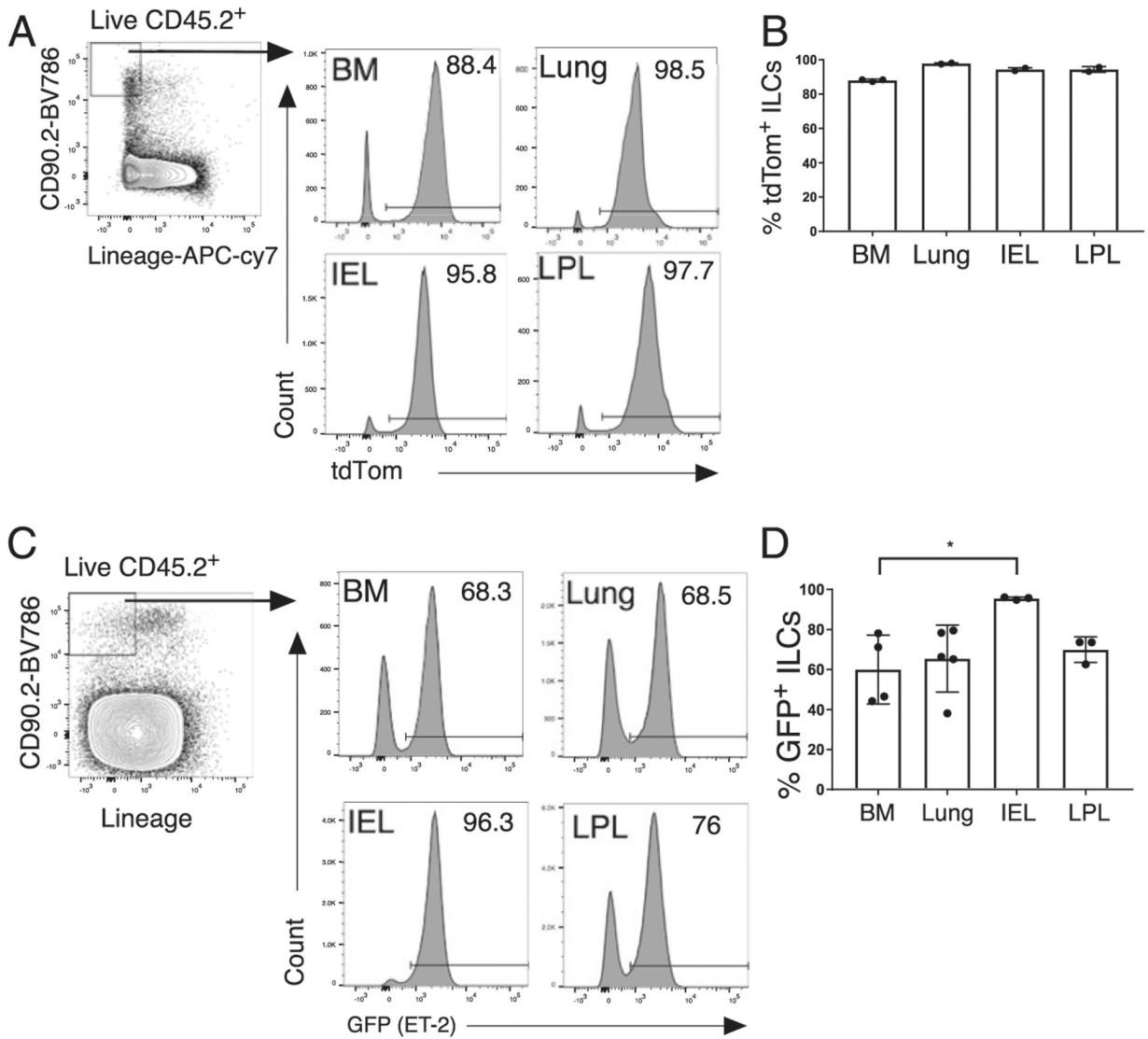


Figure 1. Sustained E protein activity negatively affects ILCs in bone marrow, lungs, and intestinal LPLs.

(A) Representative flow cytometry plots showing percentages of live CD45⁺ CD90.2⁺ Lin⁻ ILCs that are tdTomato⁺ and (B) bar graph showing percentage of tdTomato⁺ ILCs in bone marrow (BM), lung, intestinal IEL, and intestinal LPLs of Rag1-cre;tdTomato mice with each dot representing an individual mouse. (C) Representative flow cytometry plots showing percentages of live CD45⁺ CD90.2⁺ Lin⁻ ILCs that are GFP⁺ and (D) bar graph showing percentage of GFP⁺ ILCs in BM, lung, IEL, and LPL of ET-2 mice with each dot representing an individual mouse. Data are shown as mean ± SD. Ordinary one-way ANOVA on (B) and (D) with nonsignificant differences unmarked. **p* < 0.05.

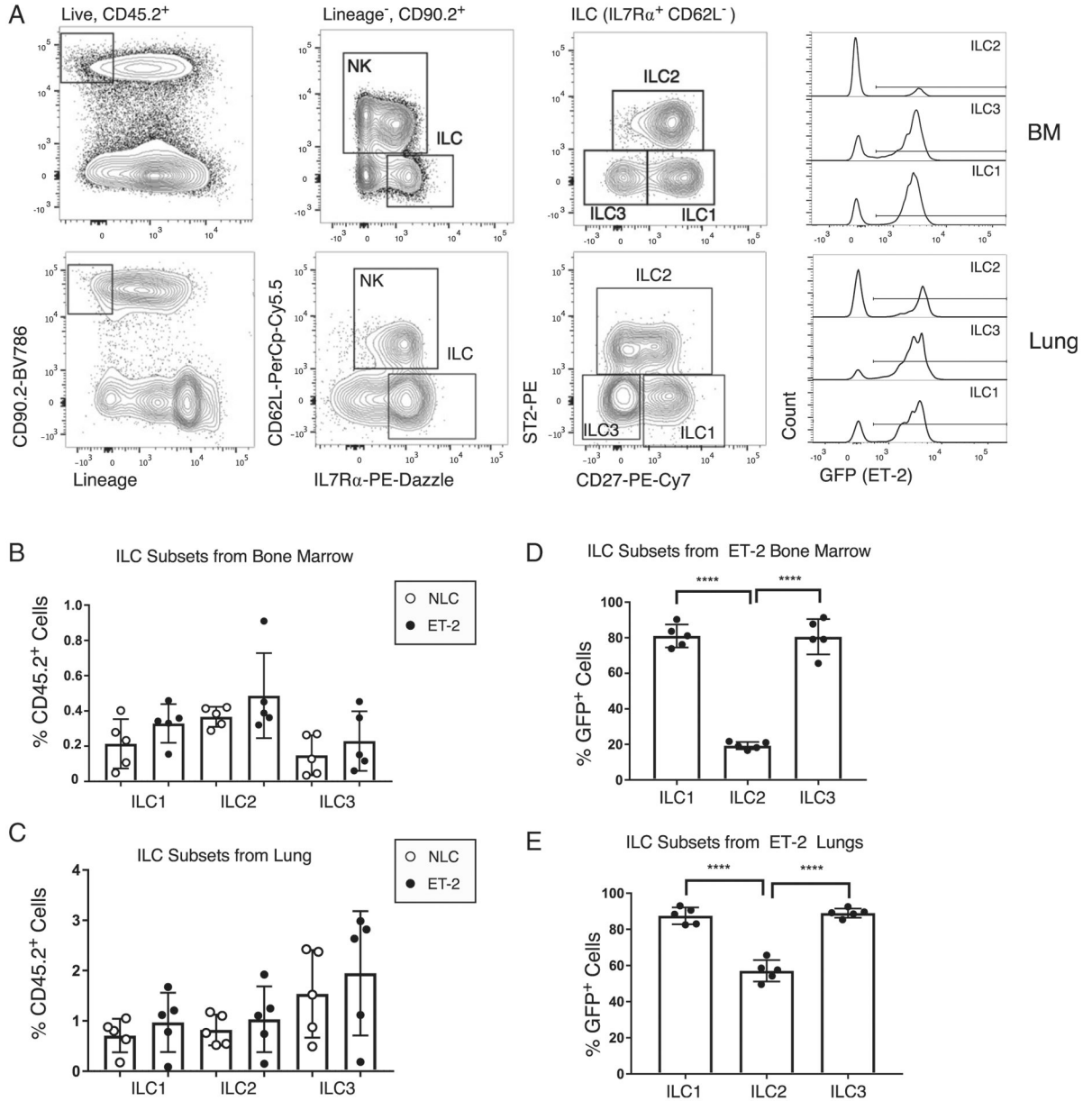


Figure 2. Sustained E protein activity negatively affects ST2⁺ CD27⁻ ILC2s. (A) Representative flow cytometry plots from ET-2 bone marrow and lung samples showing gating of live CD45.2⁺ Lin⁻ CD90.2⁺ IL-7Rα⁺ CD62L⁻ ILCs, live CD45.2⁺ Lin⁻ CD90.2⁺ IL-7Rα⁺ CD62L⁺ NKs and CD27⁺ST2⁻ ILC1s, CD27^{int} ST2⁺ ILC2s, and CD27⁻ ST2⁻ ILC3s and an overlay histogram of GFP expression within the ILC1, ILC2, and ILC3 gates. Bar graphs showing the percentage of ILC1s, ILC2s, and ILC3s in the CD45⁺ population with each dot representing an individual mouse in (B) bone marrow and (C) lung. Bar graphs showing the percentage of GFP⁺ cells in the ILC1, ILC2, and ILC3 populations with each dot representing an individual mouse in (D) bone marrow and (E) lung. Data are shown as mean ± SD. Ordinary one-way ANOVA on (B)–(E) with nonsignificant differences unmarked. *****p* < 0.0001.

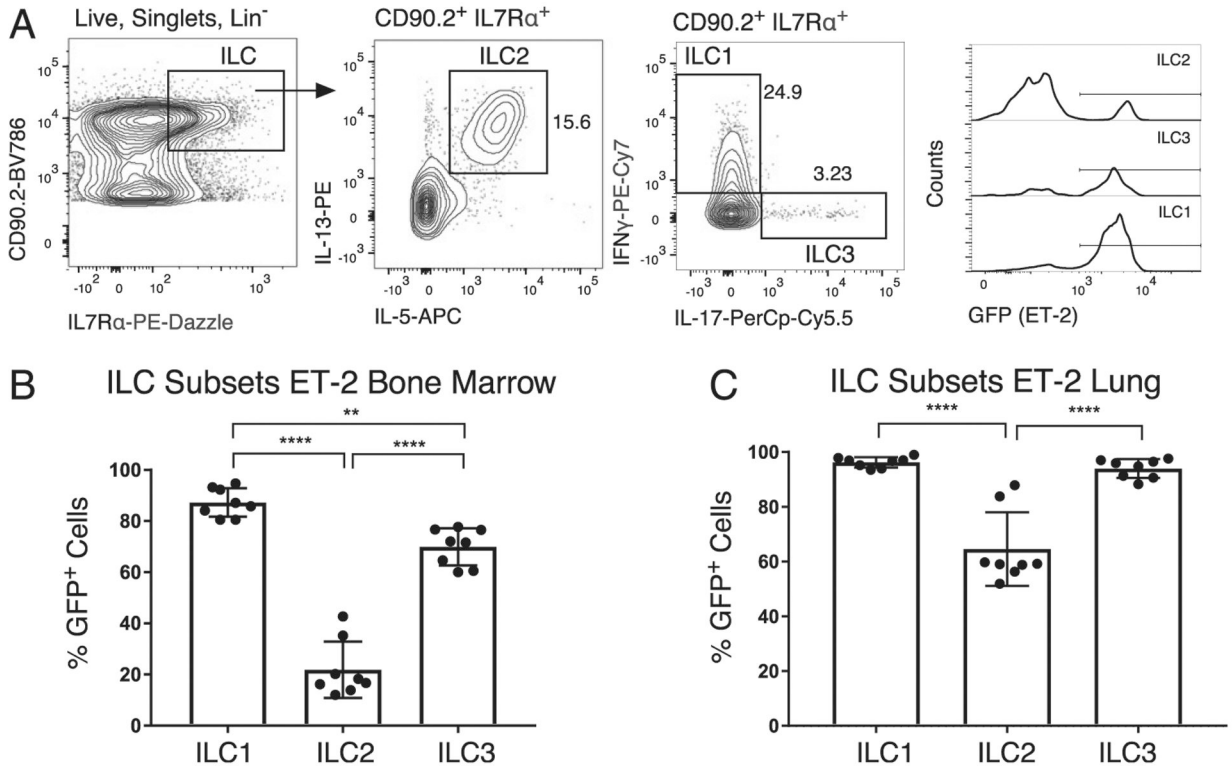


Figure 3. Sustained E protein activity negatively affects IL-5⁺ IL-13⁺ ILC2s.

(A) Representative flow cytometry plots from an ET-2 bone marrow sample stimulated with PMA and ionomycin showing gating of live CD45.2⁺ Lin⁻ CD90.2⁺ IL-7Rα⁺ ILCs, IFN- γ ⁺ ILC1s, IL-5⁺ IL-13⁺ ILC2s, and IL-17⁺ ILC3s and stacked histograms of GFP expression within the ILC1, ILC2, and ILC3 gates. Bar graphs showing the percentage of GFP⁺ cells in the ILC1, ILC2, and ILC3 populations with each dot representing an individual mouse in (B) bone marrow and (C) lung. Data are shown as mean \pm SD. Ordinary one-way ANOVA on (B) and (C) with nonsignificant differences unmarked. ***p* < 0.01, *****p* < 0.0001.

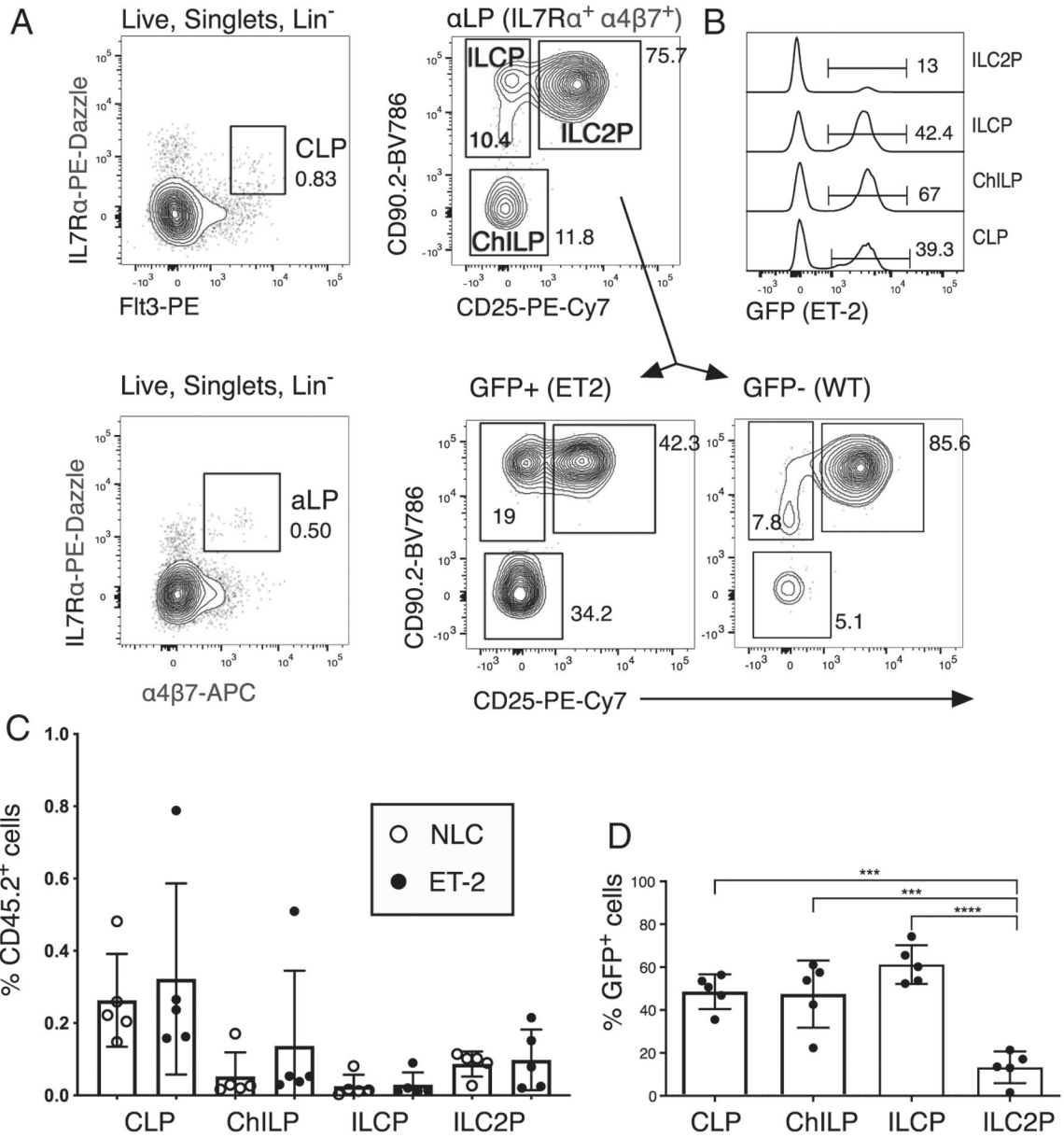


Figure 4. Sustained E protein activity negatively affects the transition from ILCP to ILC2P specific progenitors.

(A) Representative flow cytometry plots from a bone marrow sample showing gating of the ILCPs CLPs (live Lin⁻ IL-7Rα⁺ Flt3⁺), αLPs (live Lin⁻ IL-7Rα⁺ α4β7⁺), ChILPs (live Lin⁻ IL-7Rα⁺ α4β7⁺ CD90⁻ CD25⁻), ILCPs (live Lin⁻ IL-7Rα⁺ α4β7⁺ CD90⁺ CD25⁻), and ILC2Ps (live Lin⁻ IL-7Rα⁺ α4β7⁺ CD90⁺ CD25⁺). The profiles of GFP⁺ and GFP⁻ αLP are also shown. (B) An offset histogram of GFP expression within these populations. (C) Bar graph showing the percentage of bone marrow CLPs, ChILPs, ILCPs, and ILC2Ps in the CD45⁺ population of NLC and ET-2 mice. Each dot represents an individual mouse. (D) Bar graph showing the percentage of GFP⁺ cells in CLPs, ChILPs, ILCPs, and ILC2Ps in ET-2 mice. Each dot represents an individual mouse. Data are shown as mean ± SD. Ordinary

one-way ANOVA on (C) and (D) with nonsignificant differences unmarked. *** $p < 0.001$,
**** $p < 0.0001$.

Author Manuscript

Author Manuscript

Author Manuscript

Author Manuscript

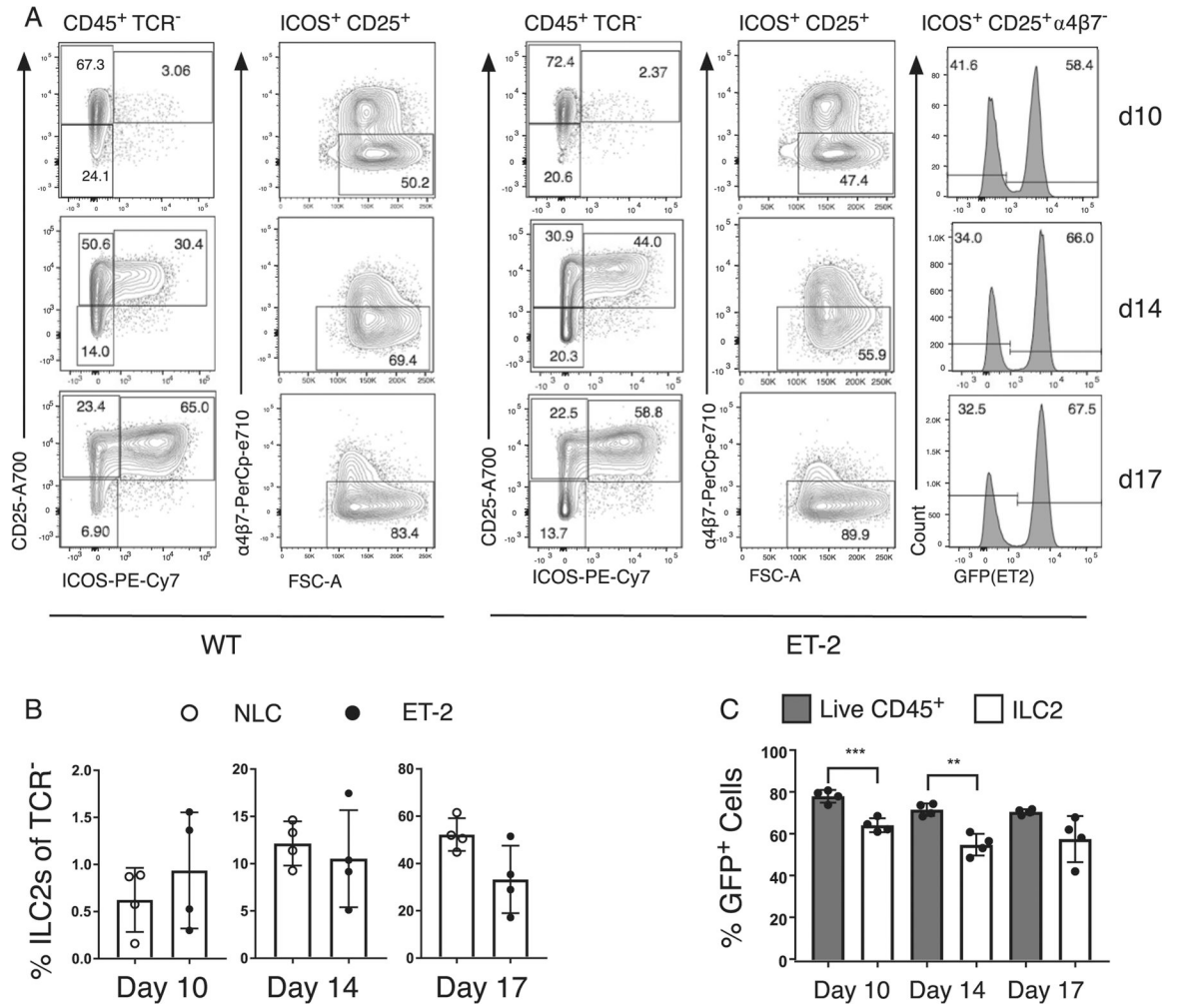


Figure 5. Sustained E protein activity negatively affects ILC2 development in vitro. (A) Representative flow cytometry plots showing CD45⁺ TCR^β⁻ TCR^γ^δ⁻ ICOS⁺ CD25⁺ α4β7⁻ ILC2s on days 10, 14, and 17 after plating wild-type (WT) or ET-2 CLPs on OP9-DL1. For the ET-1 mice, the percentage of GFP⁺ ILC2s is shown on a histogram. (B) Bar graph showing the percentage of ILC2s in the population of TCRα^β⁻ TCRγ^δ⁻ cells, and (C) the percentage of GFP⁺ cells in the live CD45⁺ population, represented by gray bars, compared with the ILC2 population, represented by white bars. Each dot represents the mean of four technical replicates with NLC mice represented by hollow circles and ET-2 mice represented by solid circles. Data are shown as mean ± SD. Unpaired *t* test on (B) and (C) with nonsignificant differences unmarked. ***p* < 0.01, ****p* < 0.001.

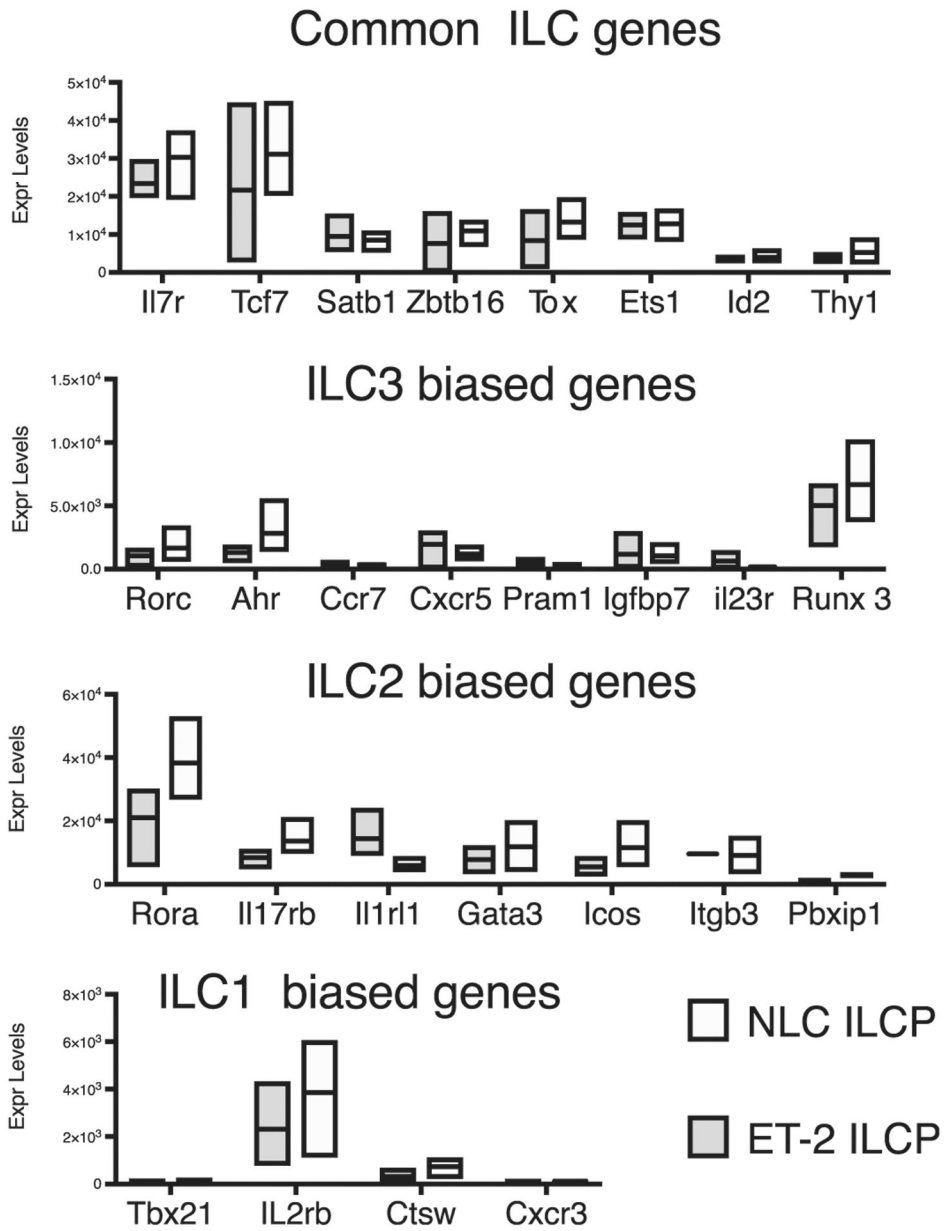


Figure 6. Expression levels of selected genes from GFP⁺ ILCs from ET-2 mice and NLC ILCs determined by RNA-seq.

GFP⁺ ILCs from ET-2 mice and ILCs from NLCs were sorted from four pooled mice in triplicate. The expression levels of selected genes known to be important for the development of ILCs is shown as floating boxes (minimum to maximum, with line at mean). None of these differences were scored as significant by the DESeq2 package.

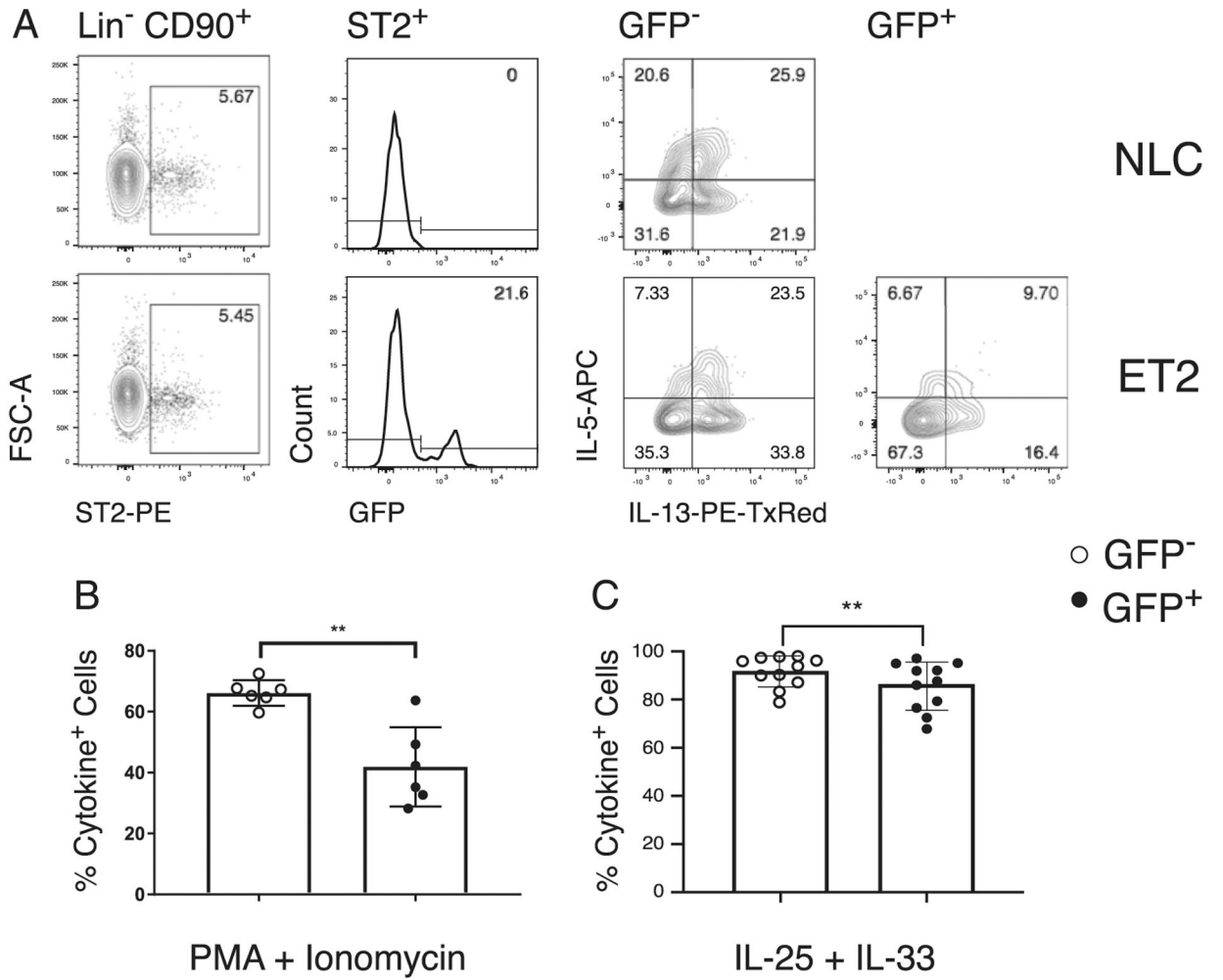


Figure 7. Sustained E protein activity affects ILC2 function.

(A) Representative flow cytometry plots from NLC and ET-2 bone marrow samples stimulated with PMA and ionomycin showing gating of live CD45.2⁺ Lin⁻ CD90⁺ ST2⁺ ILC2s and the production of IL-5 and IL-13 in both GFP⁻ and GFP⁺ ILC2s. (B) Bar graphs showing the percentage of cells producing IL-5 alone, IL-13 alone, or both cytokines together in GFP⁻ and GFP⁺ ILC2s in bone marrow. (C) Bar graphs showing the percentage of cells producing IL-5 alone, IL-13 alone, or both cytokines together in GFP⁻ and GFP⁺ ILC2s treated with IL-25 + IL-33 for 72 h. Each dot represents an individual mouse. Data are shown as mean ± SD. Paired *t* test with nonsignificant differences unmarked. ***p* < 0.01.